

Quantitative analysis on tongue inspection in traditional Chinese medicine using optical coherence tomography

Haixin Dong
Zhouyi Guo
Changchun Zeng
Huiqing Zhong

South China Normal University
Ministry of Education Key Laboratory of Laser
Life Science
Laboratory of Photonic Traditional Chinese Medicine
Guangzhou 510631, China

Yonghong He

Tsinghua University
Graduate School at Shenzhen
Shenzhen 518055, China

Ruikang K. Wang

Oregon Health and Science University
Department of Biomedical Engineering
Beaverton, Oregon 97006

Songhao Liu

South China Normal University
Ministry of Education Key Laboratory of Laser
Life Science
Laboratory of Photonic Traditional Chinese Medicine
Guangzhou 510631, China

1 Introduction

Traditional Chinese medicine (TCM) is a unique part of the glorious culture of China, which has a history of over 2000 yr and stands as an indispensable part of the medical science of the world. Tongue inspection (TI) is one of most important diagnostic methods^{1,2} of TCM. TI is based on observing any abnormal changes in the tongue to diagnose disease. Clinical data have shown significant connections between various diseases and abnormalities of the tongue.³ The content to be observed includes the color, shape, and the movement of tongue body, as well as the color, thickness of the tongue coating, and the moisture degree of the tongue. Compared with other diagnostic methods, the advantages of TI lie in its noninvasiveness and simplicity.

However, traditional TI has its inevitable deficiency; the clinical accuracy of TI is highly determined by the experience and knowledge of the physicians. For example, the thickness of the observed tongue coating is classified as thick or thin, but no value is provided for reference. It is, therefore, necessary to build an objective and quantitative diagnostic standard for TI.

Abstract. Tongue inspection (TI) is an important and unique diagnostic method in traditional Chinese medicine (TCM), because significant connections between various viscerae diseases and abnormalities in the tongue have been verified. In TCM, TI is simple and non invasive, but in clinical applications, TI is subjectively based on the experience and technique of physicians. To avoid this problem, optical coherence tomography (OCT) imaging is introduced here for TI. We study OCT imaging in rats *in vivo* from chronic gastritis group (model) and normal group (control) and quantitatively analyze the relative parameters, such as the thickness and the moisture degree of TI. Our results show that OCT images properly demonstrate the thickness of the tongue coating and the moisture degree of the tongue in both groups, and the thickness is increased in the model group from that in the normal group, while the moisture degree decreases. As a result, OCT technology has the potential to provide physicians with an objective diagnostic standard for visual TI in TCM clinical practice and research.

© 2008 Society of Photo-Optical Instrumentation Engineers. [DOI: 10.1117/1.2870175]

Keywords: optical coherence tomography; tongue inspection; tongue coating; microstructure; moisture degree.

Paper 07010SSRR received Jan. 31, 2007; revised manuscript received Oct. 15, 2007; accepted for publication Nov. 15, 2007; published online Feb. 26, 2008.

To resolve the mentioned problems, recently significant efforts have been made by several scientific groups and companies, and some new methods and systems for objectifying TI have been developed.⁴⁻¹⁴ Most researchers analyzed the color and texture of the patient's tongue based on the tongue image by computer. Previous researchers have paid more attention to collecting the TI color. The extraction of the color features can be performed in different color spaces, which usually include RGB, HSV, CIEY_{xy}, CIELUV, and CIELAB. Color space is often used in software systems to aid the interactive selection and manipulations of tongue color, and some studies have extended the color space to the IR or UV wave band. Meanwhile, other characteristics of TI are deduced by the color of the tongue body and tongue coating, Chiu et al.,¹⁵ Chiu,¹⁶ and Guo and Wang¹⁷ concretely accounted for the thickness of tongue coating through different theories. However, with these studies it remains difficult to quantify the parameters of TI *in vivo*, and almost no research on observing the glossal microstructure in depth *in vivo* has been performed.

Optical coherence tomography^{18,19} (OCT) is a recently developed and noninvasive imaging technique that provides high-resolution cross-sectional images of the microstructures

Address all correspondence to: Changchun Zeng, Laboratory of Photonic Traditional Chinese Medicine, MOE Key Laboratory of Laser Life Science, South China Normal University, Guangzhou 510631, P.R. China. Tel: +86 20-85213897-8611; Fax: +86 20-85210889; E-mail: gzzysys@scnu.edu.cn.

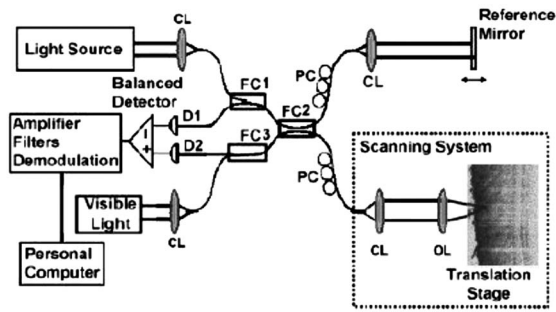


Fig. 1 Schematic of the OCT system: CL, collimating lens; FC, fiber coupler; PC, polarization controller; OL, objective lens; and D, detector.

of biological tissue. It combines the advantages of interferometers and confocal microscopy to probe the weakly backscattered photons from the microstructures beneath tissue surfaces. It has been applied *in vivo* in medical imaging and diagnostics with great success, for example in ophthalmic,²⁰ gastrointestinal,²¹ gynecological,²² dermatological,²³ and cardiological²⁴ imaging studies. The capabilities of OCT at penetration depths have also been investigated in tissues where structural information is distributed over many millimeters.

In a previous study, we investigated the feasibility of using an OCT imaging system as a method for glossoscopy,²⁵ and this method for TI was first presented by comparing the OCT image of the tongue with the histology of corresponding tissue. The aim of this study was to observe the changes in OCT images of the tongues of normal control rats and those with chronic gastritis *in vivo* and to quantify the TI parameters by detecting the thickness of the tongue coating and the degree of moisture of the tongue and then analyzing the discrepancy between the normal control and model groups.

2 Materials and Method

2.1 OCT System

Figure 1 shows a schema of the OCT system used in this study.²⁶ Briefly, a broadband light source is a superluminescent diode with a central wavelength at 1310 nm and a bandwidth of 50 nm. The light is delivered via a single-mode fiber with a mode field diameter of 5.3 μm . This OCT system provides an axial resolution of 10 to 15 μm . The transverse resolution of the system is about 25 μm , as determined by the focal spot size produced by the probe beam. The signal-to-noise ratio (SNR) of this system is measured at 100 dB. A visible light source ($\lambda=645$ nm) was used to guide the probe beam. The OCT system operation is controlled automatically by computer. The detector current is demodulated using a lock-in amplifier and a low-pass filter in software prior to storage. Each in-depth scanning (A-scan) consists of 10,000 data points. The lateral scanning (B-scan) image is obtained by moving the mirror relative to the tissue sample, which takes about 1.0 s. The data acquisition software is written in LabVIEW 7.2-D. OCT images are obtained in each experiment and stored in the PC for further processing.

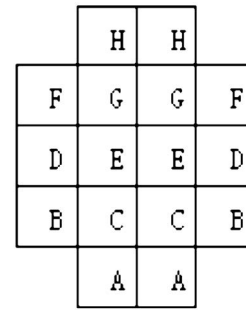


Fig. 2 Regions of the rat's tongue from A to H; A belongs to the tongue tip, which accounts for 1/5 of the tongue, B to G belong to the tongue middle, 3/5; and H belongs to the tongue root, 1/5.

2.2 Animals

Twenty female Sprague-Dawley rats, from the Laboratory Animal Center, Guangzhou University of Traditional Chinese Medicine, weighing between 150 and 200 g were used in this study. The animals were maintained in a standard laboratory, where chow and tap water were available *ad libitum* for 7 days, and then they were randomly divided into the model group ($n=10$) and the normal control group ($n=10$).

In the model group, a standard chronic gastritis (Spleen-stomach Damp-heat syndrome in TCM) rat model was used.^{27,28} Briefly, 10 rats of the model group were fed with a high-fat and sugar diet under a damp-heat environment and appropriate alcohol and axunge were alternatively perfused. The normal control group was perfused equivalent physiological saline every day and maintained in a standard environment. All rats were fed continuously for 3 weeks.

2.3 Experimental Procedure

Prior to performing the imaging, rats were anesthetized using 1% pentobarbital sodium (40 mg/kg), and then each rat was put on an optical table with its mouth widely opened by forceps and 12 positions from regions A to H (Fig. 2) on the tongue surface were scanned by OCT. Each position was scanned more than twice, and all OCT images were stored in a computer.

Histology was obtained immediately following the experiments. The rats were deeply anesthetized with pentobarbital sodium (100 mg/kg). The rat tongues were extracted and fixed in 100 ml/L neutral formalin. The sample was dehydrated with ethanol, embedded in paraffin, sectioned and stained with hematoxylin and eosin (H & E) on a glass slide. The slide was examined under an optical microscope for the structure of the tongue.

2.4 Measurement of the Thickness of the Tongue Coating

In an OCT measurement, the measured value of microstructure thickness is not the real thickness, it is the optical thickness ($l=nt$), where n and t are the refractive index and real thickness of the sample, respectively. The refractive index of biology tissues is changeable²⁹ between 1.35 and 1.45, so in this study, we chose a middle value of 1.40 as the refractive

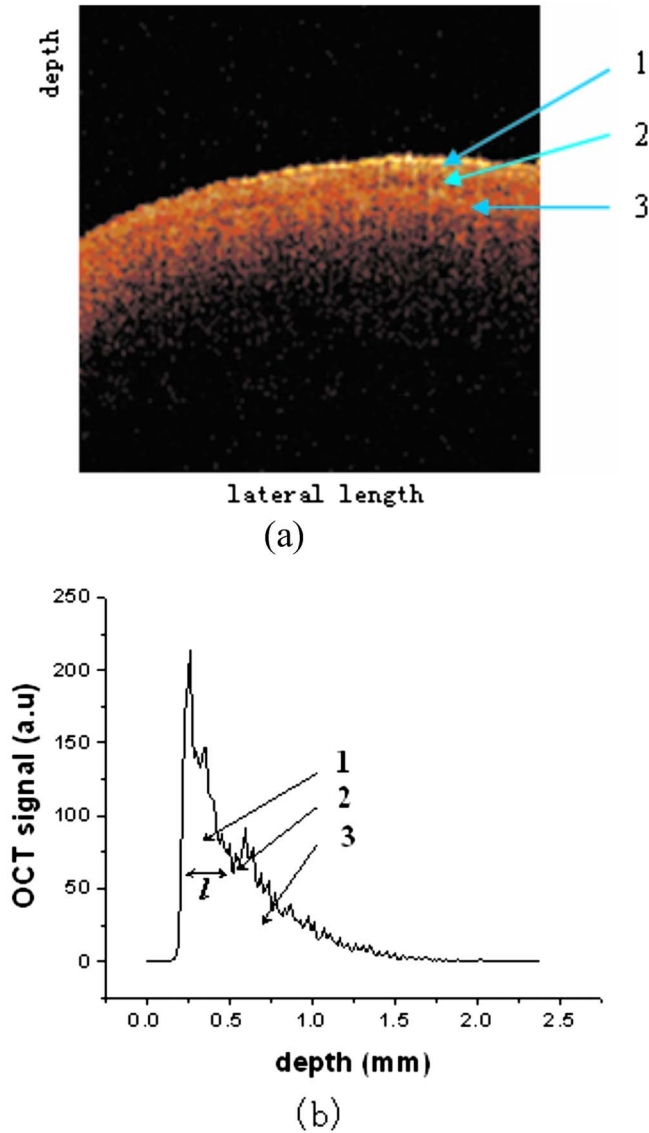


Fig. 3 (a) Typical OCT image of the normal rat's glossal surface structure and (b) corresponding 1-D OCT signal in depth: 1; tongue coating; 2, tongue body; and 3, the interface of tongue coating and tongue body.

index of the tongue coating. The optical thickness is measured, and the real thickness of the tongue coating can be determined via

$$t = l/n. \tag{1}$$

To obtain l , an average of 50 to 100 adjacent A-scans were taken from a horizontal surface of each OCT B-scan. The 2-D image was averaged into a single curve to obtain the 1-D distribution of the mean signal (or mean gray level) in depth (Fig. 3). Based on differences in the OCT signal in depth, different layers of the tongue were clearly distinguished and matched with the histology. From the results of this study, we can discern that the first layer is called the tongue coating in TCM, and l is the optical thickness of tongue coating from the depth axis.

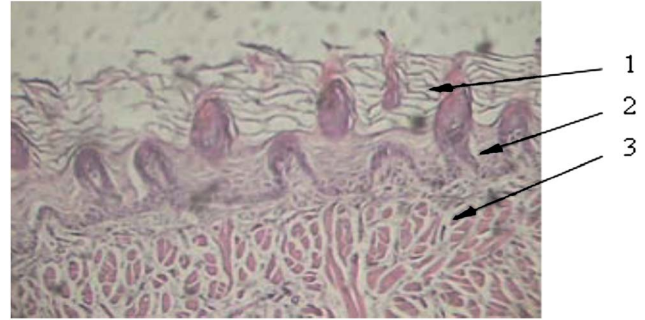


Fig. 4 Histology of the rat's normal glossal surface structure: 1, mucous stratum; 2, epithelial tissue; 3, muscular tissue.

2.5 Measurement of Moisture Degree of the Tongue

OCT imaging is based on intensity differences of backscattered light. In this model, OCT is assumed to detect only light that has been scattered once, and therefore the decay of the OCT signal with depth simply follows the Lambert-Beer law. According to the Lambert-Beer law, light attenuation inside tissues is exponential. The attenuation coefficient (μ_t) includes the scattering coefficient (μ_s) and the absorption coefficient (μ_a). Because $\mu_s \gg \mu_a$ in the near-IR spectral range, μ_t is almost proportional³⁰ to μ_s . Tissue scattering properties are highly dependent on the ratio of the refractive index of scattering centers to the refractive index of interstitial fluid, so if the interstitial fluid of the tongue, i.e., moisture degree, is changeable, the scattering properties (μ_t) should vary. In this study, the attenuation character of OCT signal within the tongue body is distinct. We used μ_t within the tongue body to assess the moisture degree of the tongue. From the 1-D distribution of the mean signal (i) in depth (d), with a Levenberg-Marquardt curve fitting algorithm, Eq. (2) is fitted to the OCT signal within the tongue body. We present OCT measurements only of the attenuation coefficient of different moisture degree tongues in region C.

$$i(d) = A \exp(-\mu_t d) + y_0. \tag{2}$$

2.6 Statistical Analysis

All values are presented as means \pm SE (standard error) for the number of samples animals. The data were analyzed by Student's t tests for unpaired data, $P < 0.05$ was the minimum accepted level of significance for all groups.

3 Results

3.1 Comparison Between OCT Image and Histology of the Normal Superficial Tongue Structure

To indicate that an OCT image can really reflect the layers of tongue coating, the OCT image and the histology information were compared. An OCT image of the normal rat's glossal surface structure is displayed in Fig. 3(a). Several fine features of the tongue are apparent. Three separate layers are clearly visible: an upper layer is the tongue coating (TC) over the glossal surface; at bottom the layer, the tongue body (TB)

Table 1 Comparison of the thickness of tongue coating.

	Number of Cases (<i>n</i>)	Tip (1/5) A (μm)	Middle (3/5)					Root (1/5) H (μm)	
			B (μm)	C (μm)	D (μm)	E (μm)	F (μm)		G (μm)
Normal control group	10	223 \pm 3	266 \pm 3	282 \pm 5	288 \pm 5	293 \pm 2	293 \pm 3	307 \pm 2	321 \pm 2
Model group	10	252 \pm 3 ^a	311 \pm 4 ^a	320 \pm 2 ^a	323 \pm 3 ^a	326 \pm 3 ^a	327 \pm 2 ^a	335 \pm 3 ^a	349 \pm 3 ^a

^a $p < 0.01$ versus normal control group.

is evident, which exhibited exponential attenuation characteristic of turbid media, and the interface between TC and TB is a darker thinner region under the scanning.

The corresponding histology is shown in Fig. 4. Three layers are also visible from the tongue tissue: the mucous stratum which is equivalent to TC, the glossal epithelial tissue, and the muscular tissue. The TB is almost completely composed of glossal muscular tissue, and the interface is composed of glossal epithelial tissue. It is shown that compared with the histology image of the tongue, the OCT scan image can clearly demonstrate the microstructure of the tongue *in vivo*.

3.2 Thickness of the Tongue Coating

The results for the thickness of tongue coating determined by OCT are presented in Table 1. From the table, we can see that the tongue thickness of the model group is much greater than that of the normal control group ($P < 0.01$). Figure 5 shows that the thickness from region A to region H has an increasing trend.

3.3 Tongue Moisture Degree

Figure 6 shows the scattering intensity of OCT signals versus the tissue depth; it is noticed that the signals decline rapidly as depth increases. Using Eq. (2) for fitting statistics, the R^2 values are 0.96775 and 0.96787 in the normal control and model groups, respectively, so both fit well with the original

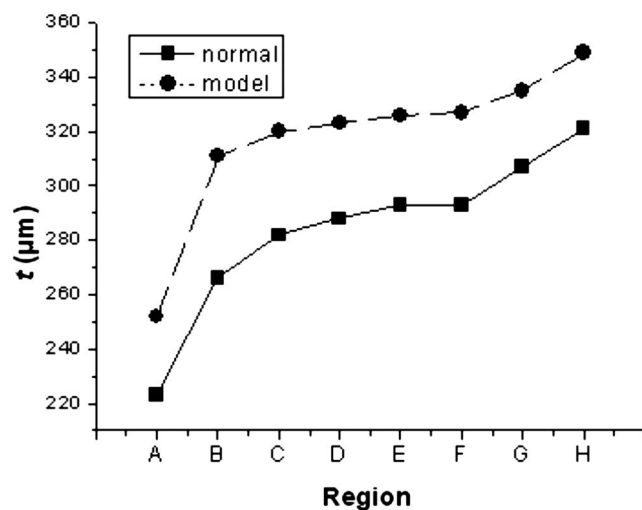


Fig. 5 Thickness of tongue coating from regions A to H. The thickness of the tongue coating shows an increasing trend from region A (tongue tip) to region H (tongue root).

curve. As described in Table 2, the μ_t value in model group is higher than that in the normal control group ($P < 0.01$). This represents the fact that the scattering property of the tongue body in model group is enhanced, and the interstitial fluid of the tongue is reduced. Thus, the moisture degree of the tongue of rats with chronic gastritis is decreased, and the discrepancy has remarkable statistical significance ($P < 0.01$).

4 Discussion

TI is an important diagnostic method in TCM practice. The thickness of the coating shows the “wax or wane of the evil and genuine,” whereas the moisture content of the body shows the “wax or wane the distribution of body fluid” in TCM. A greasy and putrid tongue, respectively, shows the retention of “dampness, phlegm, fluid or blood.” However, visual examination of a tongue is quite subjective, and its evaluation often relies on the TCM practitioner’s past experience. Therefore, an objective, noninvasive, quantitative, and *in vivo* examination method is required to help the TCM practitioner obtain tongue information from patients. The aim of this work was to obtain an objective criterion for TI using an optical method for quantitative detection of the thickness of the tongue coating, the moisture degree of the tongue, and the normal superficial tongue structure.

To validate whether an OCT image can really reflect layers of tongue coating, an OCT image and a histology figure of a normal rat’s glossal structure were compared. Our results

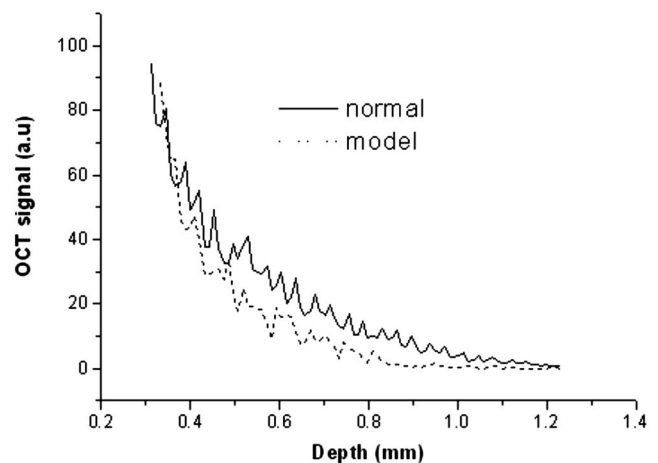


Fig. 6 Attenuation of OCT signal scattering intensity with increases in depth. The curve represents the average A-scan over the region C in an OCT image of tongue tissue (normal and model).

Table 2 The curve fit relative values in region C.

	Case (n)	Chi ² /Degrees of Freedom (DoF)	R ²	μ_t
Normal control group	10	15.23826	0.96775	4.245±0.012
Model group	10	11.26267	0.96787	7.145±0.014 ^a

^aP<0.01 versus normal control group.

showed that three separate layers are clearly visible by OCT, OCT images of different components are consistent with the histology of the tongue, and an OCT scan image can clearly demonstrate the microstructure of the tongue *in vivo*. By analyzing t and μ_t , we obtained values for the thickness of the tongue coating and the moisture degree of the tongue, and can sensitively detect the value changes in the model group and the normal control group.

Modern medical study shows that the tongue coating is made up of a keratinization tree of filiform papilla and others components (exfoliative epithelium cells, bacilli saliva, food crumbs, and leukocytes). In healthy people, the glossal epithelial cells maintain the normal formation, differentiation, exfoliative process, and relative balance. Investigation by researchers indicates that the epithelial cell development and differentiation become markedly rapid in the tongues of chronic gastritis patients, however, the cycle of exfoliation becomes relatively longer, which leads to the formation of a thick tongue coating. In our results, an increase in t of tongue in the model group is similar to the conclusions reached by the clinic inspection in TCM, and the value of the thickness of tongue coating can be provided to be combined with other diagnoses to judge the degree of gastric inflammation given in TCM. Furthermore, the moisture degree of the tongue can reflect the state of *Jin Ye*, which mainly includes blood and other fluid (liquid) in the human body in TCM. In this study, alcohol and axunge were given to rats, which harm stomachs and may lead to the reduction of *Jin Ye* in the rat tongues. This results in changes of scattering in tongues images. As a result, the moisture degree from the model group is significantly lower than that of the normal control group, and this shows that the tongues of model rats show dryness-heat and are short of *Jin Ye*, which agrees with the clinic inspection in TCM.

However, the measured t values in our study are not in a good agreement with the histology. This is possibly so for two reasons. First, the refraction of the tongue we used in this experiment is 1.40, which could be different from real refraction. Second, the discrepancy between *in vivo* and *ex vivo* layer thickness may be attributed to the shrinkage due to the fixation in the histology. In the future research, we will rank measured values in different patients according to TCM. Thus, with OCT image technology, a doctor could precisely diagnose the state of an illness by TI.

5 Conclusion

OCT was showed to be capable of imaging tongues of normal rats and rats with chronic gastritis *in vivo*. The thickness of tongue coating and the moisture degrees of the tongues could be obtained, which are important for TI in TCM. Our results show that both parameters in the model group are significantly different from those in the normal control group. This

suggests that OCT technology is capable of sensitively monitoring the changes of rat tongues, and has a potential to be developed into a useful tool to assist the TCM practitioners in diagnosis.

Acknowledgments

This project was supported in part by the National Natural Science Foundation of China (Grant No. 30600797), the Key Science and Technology Project of Guangdong Province of China (Grants No. 2004B10401031, No. 2005B50101015, and No.2006B35602001), and the Administration of Traditional Chinese Medicine Foundation of Guangdong Province of China (Grant No. 2060108).

References

1. G. Maciocia, *Tongue Diagnosis in Chinese Medicine*, Eastland Press, Seattle, WA (1987).
2. Y. Xin, X. Z. Guo, and L. S. Zhang, *Tongue Diagnosis* (Chinese-English), Tianjin Scientific and Technical Publishers, Tianjin, China (2006).
3. F. G. Yin, D. L. Tian, and C. H. Wang, "The relationship between fiber gastroscopic picture and tongue inspection," *J. Tradit. Chin. Med.* **3**(1), 49–54 (1983).
4. C. C. Chiu, "The development of a computerized tongue diagnosis system," *Biomed. Eng. Appl. Basis Commun.* **8**(4), 342–350 (1996).
5. P. C. Yuen, Z. Y. Kuang, W. Wu, and Y. T. Wu, "Tongue texture analysis using opponent color features for tongue diagnosis in traditional Chinese medicine," in *Proc. Int. Workshop on Texture Analysis in Machine Vision*, pp. 21–27 (1999).
6. T. Watsuji, S. Arita, S. Shinohara, and T. Kitade, "Medical application of fuzzy theory to the diagnostic system of tongue inspection in traditional Chinese medicine," in *Proc. IEEE Int. Conf. on Fuzzy Systems*, Vol. **1**, pp. 145–148, Seoul, South Korea (1999).
7. J. H. Zhu, P. C. Yuen, C. H. Li, Z. Y. Kuang, and W. Wu, "Towards the standardization of tongue diagnosis: an image processing approach," *Chin. J. Biomed. Eng.* **20**(2), 132–137 (2001).
8. M. G. Cui, B. Y. Xu, and S. J. Huang, "Quantitative study on tongue diagnosis in stroke patients," *Chin. J. Integr. Tradit. Western Med.* **21**(9), 670–673 (2001).
9. C. H. Li and P. C. Yuen, "Tongue image matching using color content," *Pattern Recogn.* **35**(2), 407–419 (2002).
10. J. H. Jang, J. E. Kim, K. M. Park, S. O. Park, Y. S. Chang, and B. Y. Kim, "Development of the digital tongue inspection system with image analysis," in *Proc. 2nd Joint EMBS/BMES Conf.*, Vol. **2**, pp. 1033–1034, Houston, TX (2002).
11. Y. Cai, "A novel imaging system for tongue inspection," in *Proc. IEEE Instrum. Meas. Technol. Conf.* Vol. **1**, pp. 159–163 (2002).
12. L. S. Shen, A. M. Wang, B. G. Wei, Y. G. Wang, and Z. X. Zhao, "Image analysis for tongue characterization," *Chin. J. Electron.* **12**(3), 317–323 (2003).
13. B. Pang, D. Zhang, and K. Q. Wang, "Computerized tongue diagnosis based on Bayesian networks," *IEEE Trans. Biomed. Eng.* **51**(10), 1803–1810 (2004).
14. B. Pang, D. Zhang, and K. Q. Wang, "Tongue image analysis for appendicitis diagnosis," *Inf. Sci. (N.Y.)* **175**(3), 160–176 (2005).
15. C. C. Chiu, H. S. Lin, and S. L. Lin, "A structural texture recognition approach for medical diagnosis through tongue," *Biomed. Eng. Appl. Basis Commun.* **7**(2), 143–148 (1995).

16. C. C. Chiu, "A novel approach based on computerized image analysis for traditional Chinese medical diagnosis of the tongue," *Comput. Methods Programs Biomed.* **61**(2), 77–89 (2000).
17. Z. H. Guo and K. Q. Wang, "A novel method for identifying the thickness of the tongue coating," *Chin. J. Med. Phys.* **21**(6), 332–333 (2004).
18. D. Huang, E. A. Swanson, C. P. Lin, J. S. Schuman, W. G. Stinson, W. Chang, M. R. Hee, T. Flotte, K. Gregory, C. A. Puliafito, and J. G. Fujimoto, "Optical coherence tomography," *Science* **254**, 1178–1181 (1991).
19. J. G. Fujimoto, M. E. Brezinski, G. J. Tearney, S. A. Boppart, B. E. Bouma, M. R. Hee, J. F. Southern, E. A. Swanson, and B. Bouma, "Optical biopsy and imaging using optical coherence tomography," *Nat. Med.* **9**, 970–972 (1995).
20. E. A. Swanson, J. A. Izatt, and M. R. Hee, "In vivo retinal imaging by optical coherence tomography," *Opt. Lett.* **18**(21), 1864–1867 (1993).
21. B. E. Bouma, G. J. Tearney, C. C. Compton, and N. S. Nishioka, "High-resolution imaging of the human esophagus and stomach in vivo using optical coherence tomography," *Gastrointest. Endosc.* **51**, 512–516 (2000).
22. N. D. Gladkova, G. A. Petrova, N. K. Nikulin, S. G. Radenska-Lopovok, L. B. Snopova, Y. P. Chumakov, V. Nasonova, G. V. Gelikonov, R. V. Kuranov, A. M. Swrgeev, and F. I. Feldchtein, "In vivo optical coherence tomography imaging of human skin: norm and pathology," *Skin Res. Technol.* **6**(1), 6–16 (1999).
23. G. J. Tearney, I. K. Jang, and B. E. Bouma, "Optical coherence tomography for identifying unstable coronary plaque," *Int. J. Cardiol.* **107**, 154–165 (2006).
24. M. Shakhova, F. I. Feldchtein, and A. M. Sergeev, "Applications of optical coherence tomography in gynecology," Chap. 24 in *Handbook of Optical Coherence Tomography*, B. E. Bouma and G. J. Tearney, Eds., pp. 649–672, Marcel Dekker, New York (2002).
25. H. Q. Zhong, C. C. Zeng, and Z. Y. Guo, "The early study on the inspection of tongue of the traditional Chinese medicine using optical coherence tomography," in *Proc. 5th Int. Conf. on Photonics and Imaging in Biology and Medicine (PIBM)*, pp. 6534–6365 Wu Han, China (2006).
26. Y. H. He and R. K. Wang, "Dynamic optical clearing effect of tissue impregnated with hyperosmotic agents and studied with optical coherence tomography," *J. Biomed. Opt.* **9**(1), 200–206 (2004).
27. G. H. Lu and S. X. Lao, "Establishment and evaluation of animal models of spleen-stomach damp-heat syndrome," *J. Guangzhou Univ. Tradit. Chin. Med. (in China)* **22**(3), 231–235 (2005).
28. J. Chi, J. Z. Yu, and B. Y. Fu, "Effects of alcohol and indomethacin on *Helicobacter pylori* implantation and injury of gastric mucosa," *J. China Med. Univ.* **32**(6), 517–518 (2003).
29. F. P. Bolin, L. E. Preuss, R. C. Taylor et al., "Refractive index of some mammalian tissues using a fiber optic cladding method," *Appl. Opt.* **28**(12), 2297–2303 (1989).
30. K. V. Larina, M. Motamedi, M. S. Eledrisi, and R. O. Esenaliev, "Noninvasive blood glucose monitoring with optical coherence tomography emerging treatment and technology diabetes care," *Emerg. Treat. Technol* **25**(12), 2263–2267 (2002).